JOURNAL OF CATALYSIS **139**, 513–524 (1993)

Kinetics of Carbon Formation from $CH_4 + H_2$ on Silica-Supported Nickel and Ni–Cu Catalysts

IB ALSTRUP* AND M. TERESA TAVARES†

**Haldor Topsøe Research Laboratories, Nymøllevej 55, DK-2800 Lyngby, Denmark; and †Centro de Química Pura e Aplicada (INIC), Universidade do Minho, 4719 Braga Codex, Portugal*

Received March 26, 1992; revised June 5, 1992

Steady-state rates of carbon formation on a silica-supported nickel catalyst exposed to CH_4 + H_2 gas mixtures have been measured for a range of gas compositions (partial pressure of methane, 20–80 kPa, and of hydrogen, 5–15 kPa) and temperatures in the range 723–863 K. The data are used to test various kinetic models suggested previously in the literature. It is shown that the data are in conflict with previous suggestions that the rate is, at a given temperature, solely a function of the carbon activity of the gas, but compatible with a kinetic model based on the elementary steps suggested by Grabke [Grabke, H. J., *Ber. Bunsenges. Phys. Chem.* **69**, 409 (1965)] to explain results for carbon formation on iron. However, the data cannot be explained by using the Grabke assumption that the dehydrogenation of surface methyl is rate-limiting. Also rate measurements for two silica-supported Ni–Cu catalysts with 1:99 and 1:9 Cu:Ni atom ratios, respectively, are reported. They show that the same Grabke-type kinetic model can explain the results at low carbon activity for the Ni–Cu catalysts, but that at the higher carbon activities, the rates for the $Ni_{0.9}Cu_{0.1}$ catalysts are higher than the model rates. The results for the $Ni_{0.99}Cu_{0.01}$ catalyst indicate that a small amount of Cu promotes the carbon formation. © 1993 Academic Press, Inc.

1. INTRODUCTION

Carbon formation on metals by the decomposition of carbon-containing gases has been studied for many years, mainly because of its importance in catalysis and corrosion. New promising applications, such as the production of high-quality carbon fibres and of diamond or diamond-like thin film coatings, have recently added to this interest.

The increasing utilization of natural gas, consisting mainly of methane, as an important raw material for the chemical industry makes it highly important to understand the interaction of methane with various surfaces.

The steam reforming process is the principal industrial process for converting natural gas into hydrogen or synthesis gas (*1*). A major problem in this process is to avoid carbon formation, as this can cause very serious operational problems. One way to reduce the risk and still be able to operate close to the carbon formation limit could be to dilute the nickel surface of the catalysts with atoms which are much less reactive toward CH_4 than nickel, e.g., by alloying with copper, taking advantage of the different ensemble requirements for the steam reforming and the carbon formation process (*2*).

The chemisorption of methane on nickel surfaces is observed to have a very low probability and a high activation energy (*3–5*). By molecular beam studies (*3*), it was recently shown that the chemisorption on Ni(111) is dissociative, resulting at low surface temperatures in stable CH_3 surface species, which dehydrogenate stepwise on the surface at higher temperatures.

Long ago, Grabke *et al.* (*6–8*) demonstrated that kinetic measurements of carbon deposition on α- and γ-iron surfaces exposed to CH_4 + H_2 gas mixtures could be explained quantitatively by assuming a mechanism based on stepwise dehydrogenation of surface species after chemisorp-

0021-9517/93 $5.00

tion of the methane molecule and with the dehydrogenation of methyl as the rate-limiting step. Grabke *et al.* (*9*) showed that the same kinetic model could account for measurements on iron–nickel alloys with 10 and 20 wt% nickel. Lázár *et al.* (*10*) found that the deposition of carbon on nickel foils does not obey the Grabke model at low carbon activities. They also reported that Grabke and co-workers found the rate of hydrogasification to be proportional to the hydrogen partial pressure. Figueiredo and Trimm (*11*) found the same hydrogen pressure dependence for the time-independent rate of hydrogasification of carbon on nickel foils and Ni/Al_2O_3 catalysts. Moreover, they observed that in the case of nickel foils, the rate of hydrogasification was proportional to the amount of carbon initially present, while no correlation was observed in the case of the supported catalysts. Audier and Coulon (*12*) showed that the rate of carbon deposition on an iron–nickel catalyst with 75% nickel in both $CH_4 + H_2$ and $CO + CO_2$ mixtures depended linearly on the carbon activity a_c of the gas. Bernardo *et al.* (*13*) fitted a modified version of the Grabke kinetic expression to a small number of rates measured for carbon deposition from $CH_4 + H_2$ mixtures on silica-supported Ni–Cu catalysts. Baker *et al.* (*14*) and Rostrup-Nielsen and Trimm (*15*), on the other hand, suggested that the diffusion of carbon through the nickel particle is the rate-limiting step during the steady-state growth of carbon filaments on Ni catalysts. Recently Safvi *et al.* (*16*) studied the rate of carbon formation from $CH_4 + H_2$ gas mixtures on carbon-supported nickel catalysts and found at low a_C a smooth but curved dependence on a_C, while the rates essentially saturated above a critical a_C. Also recently Demicheli *et al.* (*17*) studied carbon formation on alumina-supported nickel catalysts from $CH_4 + H_2$ gas mixtures and found that the results could be explained by a model based on the elementary steps suggested by Grabke but with the adsorption step being rate-limiting.

In the present work we report on a study of the steady state rates of carbon deposition on silica-supported catalysts, one nickel catalyst and two nickel–copper alloy catalysts with 1 : 99 and 1 : 9 Cu : Ni atom ratios, respectively, in $CH_4 + H_2$ mixtures as a function of the partial pressures of CH_4 and H_2 and as a function of temperature. Various kinetic models are tested on these data. It is shown that the rate at constant temperature is not solely a function of the carbon activity of the gas, but that linearized versions of the Grabke-type kinetic models can be fitted accurately to the experimental results for the nickel catalyst, but only below a critical carbon activity, which depends weakly on the temperature, to the results for the $Ni_{0.9}Cu_{0.1}$ catalyst. The linearization is based on the assumptions that the coverages of the surface species, with the exception of carbon, are small and that the carbon coverage stays constant at constant temperature.

2. EXPERIMENTAL

2.1. Catalyst Preparation

The catalysts were prepared by "dry" impregnation with a 20% weight of the metallic phase. The silica support material (Cab-O-Sil H5) was mixed with an aqueous solution of $Ni(NO_3)_2 \cdot 6H_2O$ and $Cu(NO_3)_2 \cdot 3H_2O$ in the right proportion to obtain the desired molar composition of the metallic phase. The volume of the solution was equal to the measured pore volume of the support material. Three different compositions of the metallic phase were considered in the present work: 100% Ni, 1% Cu + 99% Ni, and 10% Cu + 90% Ni. The mixing gave a thick, homogeneous liquid, which was dried at room temperature and calcined at 773 K for 3 h. After addition of a plasticizer (Melhorel Dow A_4C) and water, small cylindrical pellets with 4 mm diameter and 4 mm length were extruded from the powder. The pellets were calcined for 2 h at 873 K. Finally, the catalysts were prereduced at 773 K in H_2 for 44 h.

2.2. *Characterization*

Reduced catalyst samples were characterized by hydrogen chemisorption, X-ray diffraction, and nitrogen physisorption. The nickel area of the fresh nickel catalyst calculated from the hydrogen chemisorption results was about 6 m^2/g-cat, while the X-ray diffraction peak width corresponded to an average nickel particle size of about 20 nm, in excellent agreement with results obtained previously for catalysts prepared in the same way (*13*, *18*). Also the X-ray diffraction and hydrogen chemisorption results for the Ni–Cu catalysts were in good agreement with the results obtained in Ref. (*13*), i.e., X-ray diffraction spectra of the reduced catalysts showed only one metal phase to be present and the lattice parameters corresponded closely to an alloy with the nominal composition. The hydrogen chemisorption showed that Cu was segregated to the surface of the metal particles of the reduced Ni–Cu catalysts.

2.3. *Reactor System*

The reactor system consisted of a microbalance (C. I. Electronics, MK2CT5) and associated flow reactor, furnace, flow, and temperature controllers. The temperature was measured with a chromel–alumel thermocouple placed close to the pellet. The rates of carbon deposition were determined from the slopes of the curves drawn by the microbalance recorder. High-purity gases (CH_4, H_2 and N_2, >99.95%) were used.

2.4. *Experimental Conditions*

Before each experiment the reactor and tube system were flushed with N_2. The catalysts were reduced at 753 K for 1 h in H_2 diluted with N_2 at a flow of 2×10^{-2} Nm^3 h^{-1}, $P_{H_2} = 15$ kPa. The flow rate during reaction was 2.5×10^{-4} mol s^{-1}. The conversion, determined by mass balance, was less than 5% so the reactor can be considered a differential one in the present conditions. Estimates based on this flow rate show that external diffusional restrictions are negligible. It was also verified that the reaction rate did not change when the flow rate was varied. Internal diffusion restrictions cannot be ruled out at the higher reaction rates, as indicated by a comparison between pellet activity and powder activity at 863 K and as treated further in the Discussion section. Also large amounts of carbon could give diffusional restrictions. The experimental conditions were chosen so that the weight of the carbon formed never exceeded 50% of the original sample weight.

Steady-state carbon deposition rates were measured at temperatures in the range 723 to 863 K. Most of the experiments were carried out with the abovementioned extruded catalyst pellets, but in addition a few were performed with catalyst powder made by crushing the pellets. For each temperature, a fresh catalyst was used and the partial pressures of methane and hydrogen were varied independently in the ranges 20 to 80 kPa and 5 to 15 kPa, respectively. For all three catalysts measurements were made at five pressure conditions at each of eight temperatures, while for the 100% Ni catalyst in addition rate measurements were made at 24 pressure conditions at each of the temperatures 723, 773, and 823 K. The results from the latter experiments form the basis of the kinetic modelling in the present paper and also in another paper (*19*) in which a microkinetic model is developed and discussed.

3. RESULTS

In this Section, both the experimental results and kinetic expressions are presented.

3.1. *Rate versus Carbon Activity*

In several papers (*12*, *16*, *20*, *21*), rates of carbon formation on metals at constant temperature in $CH_4 + H_2$ or $CO + CO_2$ gas mixtures or more complicated gas mixtures are presented as a function solely of the carbon activity a_C (or $RT \ln a_C$). Thus, in these papers it is tacitly assumed that other parameters need not be taken into account.

The carbon activity a_C of a $CH_4 + H_2$ gas mixture is defined by

$$a_C = K_{p1}P_{CH_4}/P^2_{H_2}$$

where K_{p1} is the equilibrium constant of the reaction

$$CH_4 \rightleftharpoons C(\text{graphite}) + 2H_2.$$

The carbon activity a_C of a CO + CO_2 gas mixture is defined by

$$a_C = K_{p2}P^2_{CO}/P_{CO_2},$$

where K_{p2} is the equilibrium constant of the Boudouard reaction

$$CO + CO \rightleftharpoons C(\text{graphite}) + CO_2.$$

Audier and Coulon (*12*) presented plots of rates of carbon formation on Fe–Ni catalysts in both CH_4 + H_2 and CO + CO_2 gas mixtures versus a_C. In both cases, a linear relation was demonstrated and the same slope was obtained in the two cases. Bianchini and Lund (*20*) presented measurements of rates of carbon formation on an iron catalyst in CH_4 + H_2 gas mixtures plotted as function of a_C at various temperatures. The plots showed that above a critical a_C, the rates became essentially independent of a_C, while at low a_C the results were similar to those obtained by Audier and Coulon although some deviations from linearity were evident. Recently, Safvi *et al.* (*16*) presented similar results for a carbon-supported nickel catalyst.

Grabke (*6–8*) showed long ago, as mentioned above, that the kinetics of carbon formation on iron catalysts in CH_4 + H_2 gas mixtures can be accurately accounted for by assuming that CH_4 is chemisorbed and dehydrogenated stepwise on the surface and that the first dehydrogenation step is rate-limiting. The Grabke results and model are thus not compatible with the assumption that the carbon formation rate depends solely on a_C at constant temperature.

The rates obtained for the Ni catalyst at 723 K in the present work are plotted versus a_C in Fig. 1. The rates obtained at 773 and 823 K give a similar scatter when plotted versus a_C. It is thus clearly demonstrated that a description of the kinetics of carbon formation based solely on a_C and the temperature as independent variables is not meaningful under our experimental conditions.

3.2. Grabke-Type Models

We use the model of Grabke (*6*) for carbon formation on iron as a starting point for the construction of a kinetic model for carbon formation on nickel. Molecular beam studies (*3*) of methane interacting with Ni(111) confirm the stepwise dehydrogenation of surface species assumed by Grabke, but indicate that no precursor is involved in the dissociative chemisorption of the methane molecule. A direct dissociative chemisorption of methane is also in agreement with the results obtained by Chorkendorff *et al.* (*5*). Therefore, we assume that the steps below are governing the rates of carbon formation on the nickel catalyst,

$$H_2 + 2* \rightleftharpoons 2H* \qquad (1)$$

$$CH_4 + 2* \rightleftharpoons CH_3* + H* \qquad (2)$$

$$CH_3* + * \rightleftharpoons CH_2* + H* \qquad (3)$$

$$CH_2* + * \rightleftharpoons CH* + H* \qquad (4)$$

$$CH* + * \rightleftharpoons C* + H* \qquad (5)$$

$$C* + ss1 \rightleftharpoons C_{b1} + * \qquad (6)$$

$$C_{b1} + ss2 \rightleftharpoons C_{b2} + ss1 \qquad (7)$$

$$C_{b2} + ws \rightleftharpoons C_w + ss2, \qquad (8)$$

where * signifies a surface site and CH_x* with x = 0–3 are chemisorbed species. C_{b1} means a carbon atom in the bulk phase of the nickel crystal at a subsurface site ss1 just below the surface on which the surface reactions take place and C_{b2} a carbon atom at a subsurface site ss2 just below the interface between the nickel particle and the carbon segregating out of the nickel particle. C_w is a carbon atom at a site ws in the final carbon phase, which in the present conditions is most likely to be a carbon filament (whisker) (*13*).

In order to be able to obtain a rate expres-

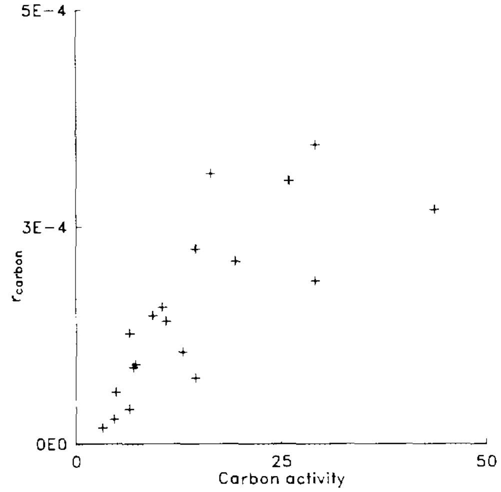

FIG. 1. Plot of the experimental rates of carbon formation at 723 K on Ni/SiO$_2$ catalyst in CH_4 + H_2 gas mixtures versus the carbon activity a_C of the gas.

sion, we make the following additional assumptions:

(i) All the steps are in quasi-equilibrium except one, which can be either step (2), the dissociative CH_4 chemisorption step, or one of the subsequent dehydrogenation steps, (3)–(5).

(ii) The surfaces species are all competing for the same surface sites and the occupation of a site is independent of the occupation of the other sites (Langmuir-type model).

The information necessary for a description of the steps (6)–(8) is not available, but is not needed because of assumption (i), which means that these steps enter the rate expression through a constant carbon coverage.

For each of the steps (2) to (5) assumed to be rate-limiting we can then derive a rate expression, which if step (2) is rate-limiting turns out to be

$$r_2 = k_2(P_{\mathrm{CH}_4}\theta*^2 - \frac{1}{K_2}\theta_{\mathrm{CH}_3}\theta_{\mathrm{H}}), \qquad (9)$$

with

$$\theta_{\mathrm{CH}_3} = \frac{a_{\mathrm{H}}^3}{K_3K_4K_5}\theta_{\mathrm{C}}, \qquad (10)$$

where

$$a_{\mathrm{H}} = \sqrt{K_1P_{\mathrm{H}_2}},$$

and if step (3) is rate-limiting the expression

$$r_3 = k_3(\theta_{\mathrm{CH}_3}\theta* - \frac{1}{K_3}\theta_{\mathrm{CH}_2}\theta_{\mathrm{H}}) \qquad (11)$$

is obtained with

$$\theta_{\mathrm{CH}_3} = \frac{K_2}{a_{\mathrm{H}}}P_{\mathrm{CH}_4}\theta*, \qquad (12)$$

where K_n, n = 1–5, are equilibrium constants of steps (1) to (5) and k_2 and k_3 are rate constants of the forward rate of step (2) and (3), respectively. $\theta*$ is the concentration of unoccupied sites, i.e.,

$$\theta* = 1 - \theta_{\mathrm{H}} - \theta_{\mathrm{CH}_3} - \theta_{\mathrm{CH}_2} - \theta_{\mathrm{CH}} - \theta_{\mathrm{C}}, \qquad (13)$$

where θ_x is the concentration of sites occupied by species x. θ_x is calculated from equilibrium expressions corresponding to steps (1), (5), and (4) for x = H, x = CH, and x = CH_2, respectively:

$$\theta_{\mathrm{H}} = a_{\mathrm{H}}\theta*, \quad \theta_{\mathrm{CH}} = \frac{a_{\mathrm{H}}}{K_5}\theta_{\mathrm{C}}, \quad \theta_{\mathrm{CH}_2} = \frac{a_{\mathrm{H}}}{K_4}\theta_{\mathrm{CH}}.$$

Expressions similar to (9) and (11) are easily derived assuming one of the steps (4) or (5) to be rate-limiting. A consequence of the assumption of quasi-equilibrium is, as mentioned above, that θ_C stays almost constant irrespective of the hydrogen and methane pressures. If we assume that the coverages of the other surface species are negligible the expressions (9) and (11) can be transformed into expressions linear in x, where

$$x = \frac{P_{\mathrm{CH}_4}}{P_{\mathrm{H}_2}^2}.$$

The dependent variables are

$$\frac{r_2}{P_{\mathrm{H}_2}^2} \quad \text{and} \quad \frac{r_3}{P_{\mathrm{H}_2}^{3/2}},$$

respectively.

The experimental results obtained for the

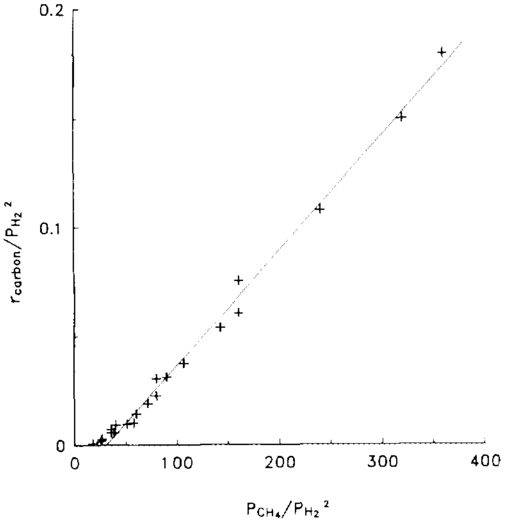

FIG. 2. Experimental rates of carbon formation on the Ni/SiO$_2$ catalyst in CH$_4$ + H$_2$ gas mixtures at 723 K compared with the linearized kinetic model with the CH$_4$ chemisorption step being rate-limiting.

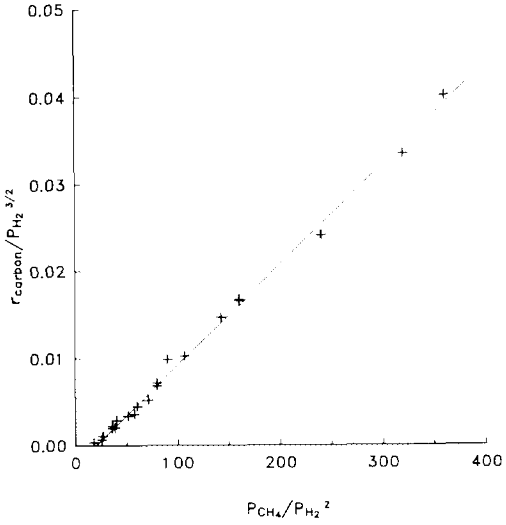

FIG. 3. As Fig. 2, except that the dehydrogenation of surface methyl is assumed to be rate-limiting.

Ni catalyst at 723 K are plotted in Figs. 2 and 3 in accordance with the linearized Grabke-type model based on the above assumptions and with step (2) or (3) as the rate-limiting step, respectively.

Plots corresponding to either step (4) or step (5) as rate-limiting do not give a similar good agreement. The plot corresponding to step (5) being rate-limiting is shown in Fig. 4. Thus we conclude that it is highly probable that either step (2) or step (3) is rate-limiting or that none of them can be considered to be close to equilibrium.

Plots of the results for the Ni catalyst at 773 K corresponding to step (3) or step (2) being rate-limiting are shown in Fig. 5 and Fig. 6, respectively. In this case only the latter plot gives a linear dependence. Figure 7 shows the results for the Ni catalyst at 823 K plotted in accordance with the linearized model with step (2) being rate-limiting. The results are in good agreement with a straight line plot. It thus appears that the latter model gives good agreement with the data for the Ni catalyst at all three temperatures.

The same model is used in Fig. 8 to compare results for the Ni catalyst with results obtained at the same conditions for the Ni$_{0.9}$Cu$_{0.1}$ and Ni$_{0.99}$Cu$_{0.01}$ catalysts. The results for the Ni$_{0.9}$Cu$_{0.1}$ catalyst give linear plots at the temperatures 723–823 K only at carbon activities lower than a critical one which depends on temperature. The ob-

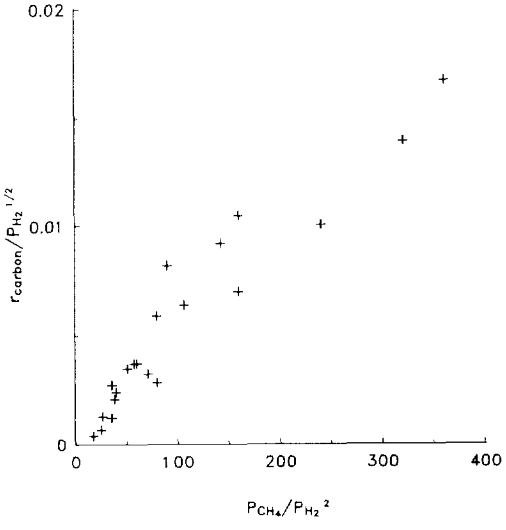

FIG. 4. As Fig. 2, except that the dissociation of surface CH is assumed to be rate-limiting.

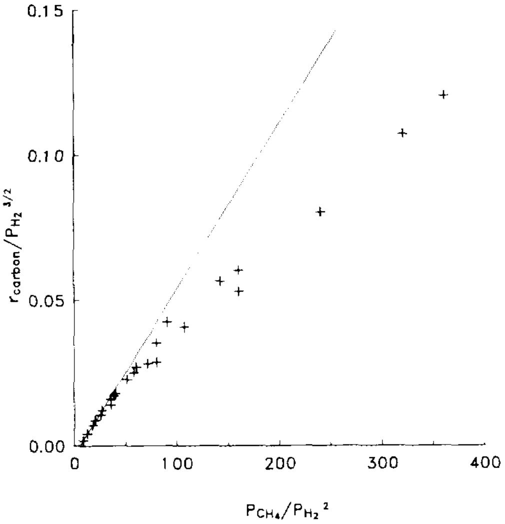

FIG. 5. As Fig. 3, except that the rates are measured at 773 K.

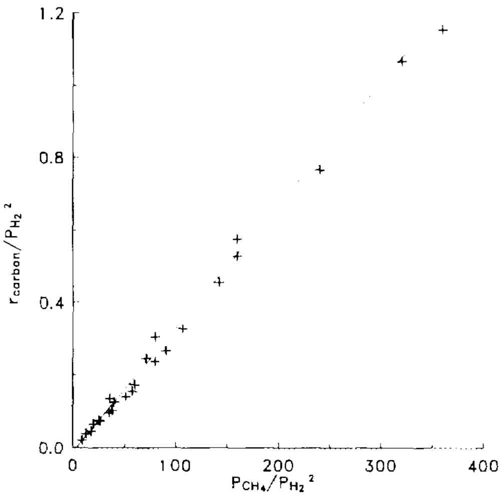

FIG. 7. As Fig. 2, except that the rates are measured at 823 K.

served rate is significantly higher than the model rate at activities higher than the critical one. The rate results for the $Ni_{0.99}Cu_{0.01}$ catalyst are all above the results for the Ni catalyst indicating that a small addition of Cu enhances the rate of carbon formation.

Figure 9 shows an Arrhenius plot of the slopes of the linearized model corresponding to step (2) being rate-limiting fitted to the results for the Ni catalyst and to the low a_C results for the $Ni_{0.9}Cu_{0.1}$ catalyst. The slopes of the Arrhenius lines correspond to an activation energy for $k_2\theta^{*2}$ of about 90 kJ/mol for both the Ni catalyst and the $Ni_{0.9}Cu_{0.1}$ catalyst.

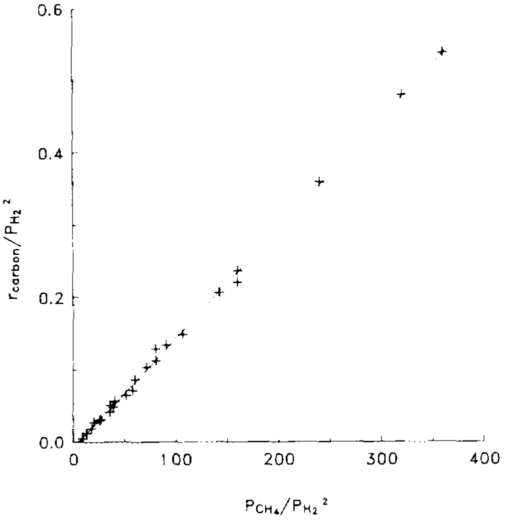

FIG. 6. As Fig. 2, except that the rates are measured at 773 K.

4. DISCUSSION

The results plotted in Fig. 1 clearly show that the practice used by several authors (*12, 16, 20, 21*) of plotting rates of carbon formation at constant temperature T versus the carbon activity a_C of the gas is misleading as it cannot in general be assumed that the rate for a given catalyst is only a function of T and a_C. In some cases, a fortuitous cancellation may take place making such an assumption valid within a limited range of reaction conditions. For instance, if in the Grabke-type kinetic model the hydrogen coverage is not small we have

$$\theta^* \approx (1 - \theta_C)/(1 + (K_1 P_{H_2})^{1/2})$$

and if $K_1 P_{H_2} \gg 1$, which might be the case at high hydrogen pressures and/or if the hydrogen chemisorption bond is stronger than on nickel, and if the chemisorption of CH_4 requires four empty sites, which is reasonable to assume (*5*), then the model with the rate limited by step (2) gives

$$r_2 = k_2\left(P_{\mathrm{CH_4}} - \frac{a_{\mathrm{H}}^4\theta_{\mathrm{C}}}{K_2K_3K_4K_5}\right)\theta*^4$$

or

$$r_2 = (k_2/(K_{\mathrm{p1}}K_1^2))a_{\mathrm{C}} - \text{constant.}$$

However, obviously this cancellation does not take place for carbon formation on nickel in our conditions nor for carbon formation on iron or iron–nickel alloys in the conditions used by Grabke *et al.* (*6–9*). Also in the abovementioned papers (*12, 16, 20, 21*) in which the carbon formation rate has been plotted versus a_{C}, such a cancellation has not been demonstrated and is not likely under the conditions used.

The Grabke-type kinetic models considered were linearized in order to be able to compare them easily and reliably with experimental results. The two main assumptions made are that only one step deviates from equilibrium and that all the coverages with the exception of the carbon coverage were small. The excellent agreement obtained makes the model plausible but does not prove the validity of the assumptions. The fact that the plots in Fig. 2 and Fig. 3 do not allow us to decide whether step (2) or step (3) is rate-limiting at 723 K might indicate that both of these steps deviate from equilibrium. A more general model is thus required to test the assumptions. This means, however, that more parameters have to be introduced, making the fitting procedure difficult and ambiguous. However, the number of parameters to be fitted to the data at one temperature can be reduced to essentially the two rate constants k_2 and k_3 by treating a more general model, in which step (2) and step (3) are allowed to deviate from equilibrium, as a microkinetic model, i.e., by calculating the equilibrium constants of all the steps by using available information about vibration and chemisorption bond energies of the surface species for a steady-state model. As the activation energy of k_2 is known for nickel single-crystal surfaces from surface science experiments (*4, 5*) only one parameter, k_3, has to be adjusted at other temperatures. The construction of such a more general microkinetic model has been carried out by the present authors and is discussed in another publication (*19*). This microkinetic model gives excellent agreement with the data obtained at 723 K. The agreement with the data obtained at 773 and 823 K is also quite good, although small, one-sided differences between model rates and experimental rates are observed at the higher rates. We suggest that these deviations may be due to the influence of a finite rate of gas diffusion through the pellet and/or to deactivation at the high rates where more carbon has been accumulated. The suggestion that diffusion restrictions may play a role is supported by estimates of the effective methane diffusion coefficient for the catalyst pellet, indicating that Knudsen diffusion is dominating. This means that a significant drop in methane concentration may be present in the pellet at the higher rates. An experiment was carried out in which the carbon formation rates were measured at 863 K on the Ni catalyst in the form of powder, produced by crushing pellets, and compared with rates measured at the same conditions on pellets of the Ni catalyst. The rates were between 20 and 25% lower on the pellets than on the powder indicating diffusion restrictions. However, it should be kept in mind that the enhancement obtained by crushing the pellet could

---

FIG. 8. Experimental rates of carbon formation on Ni/SiO_2 (○), $Ni_{0.9}Cu_{0.1}/SiO_2$ (+), and $Ni_{0.99}Cu_{0.01}/SiO_2$ (□) catalysts in $CH_4 + H_2$ gas mixtures compared with the linearized kinetic model with the CH_4 chemisorption step being rate-limiting: (a) 723 K, (b) 763 K, (c) 823 K, (d) 843 K, and (e) 863 K.

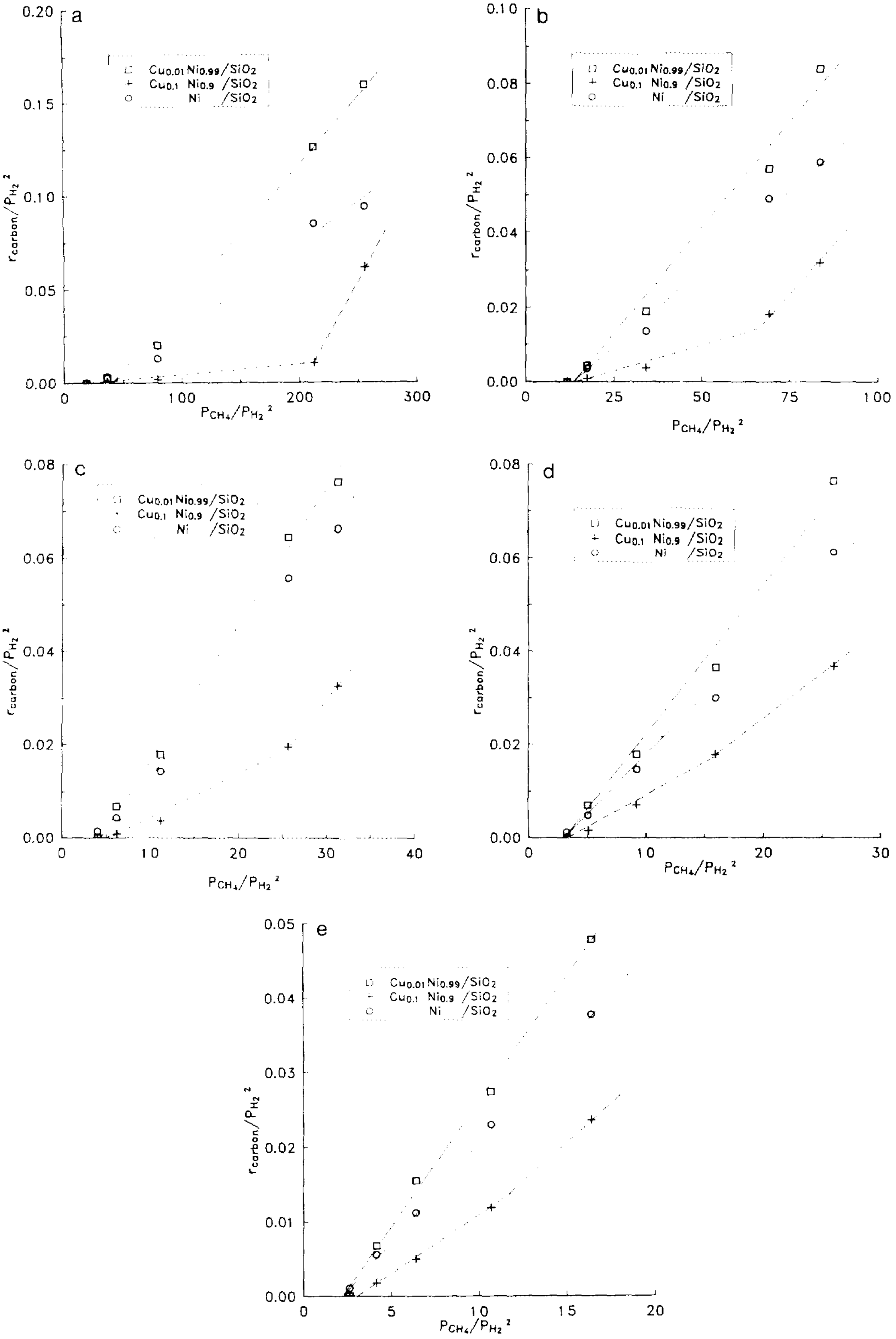
a
b
c
d
e
$Cu_{0.01}Ni_{0.99}/SiO_2$
$Cu_{0.1}Ni_{0.9}/SiO_2$
Ni/SiO_2
$r_{carbon}/P_{H_2}^2$
$P_{CH_4}/P_{H_2}^2$
0.20
0.15
0.10
0.05
0.00
0
100
200
300
0.10
0.08
0.06
0.04
0.02
0.00
0
25
50
75
100
0.08
0.06
0.04
0.02
0.00
0
10
20
30
40
0.08
0.06
0.04
0.02
0.00
0
10
20
30
0.05
0.04
0.03
0.02
0.01
0.00
0
5
10
15
20

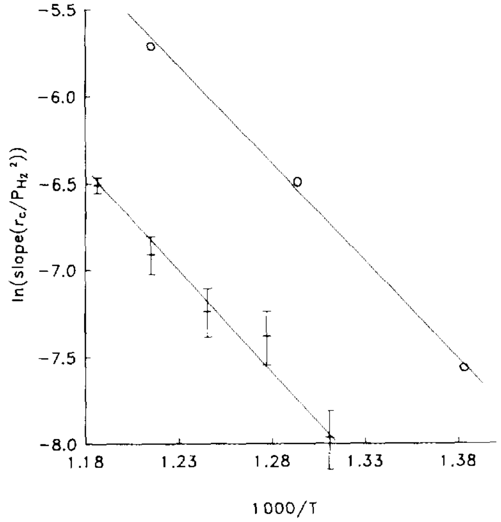

FIG. 9. Arrhenius plots of the slopes of $r_c/P_{H_2}^2$ for the Ni/SiO$_2$ catalyst (○) from Figs. 2, 6, and 7 and of the slopes for the $Ni_{0.9}Cu_{0.1}/SiO_2$ catalyst (+) from the straight lines corresponding to the low rates on the $Ni_{0.9}Cu_{0.1}/SiO_2$. The two linear regression lines both correspond to an activation energy of about 90 kJ/mol for $k_2\theta*^2$.

partly or entirely be due to the creation of new active sites by the crushing.

The microkinetic modelling (*19*) shows that neither step (2) nor step (3) are close to equilibrium in the entire range of experimental conditions. It also shows that the assumption that the coverages of all the surface species except carbon are small is quite well fulfilled except at the highest hydrogen pressures, which corresponds to the lowest rates, where in any case the measurements are least accurate. It would clearly be better to improve the linearized models by keeping the hydrogen coverage in the $\theta*$ expression, i.e., by introducing the equilibrium constant K_1 as a separate, free parameter to be adjusted in a nonlinear fitting as done by Demicheli *et al.* (*17*). However, such an improvement would not help us to solve the problem of which steps are deviating from equilibrium.

It is interesting to note that the $Ni_{0.9}Cu_{0.1}$ catalyst at low a_C values has rates which depend on partial pressures in accordance with the Grabke-type model but are only a fraction (~12% at 723 K) of the rates of the Ni catalyst at the same conditions, while at higher a_C values the rate differences between the two catalysts are much smaller. A similar change in the kinetic behavior as a function of a_C was observed by Bernardo *et al.* (*13*). They modelled only the high a_C region of the data and suggested that the deviation from the model at the lower a_C values (higher P_{H_2}) was due to saturation of the backward gasification reaction. A consequence of this explanation, however, would be that the equilibrium of the carbon formation on the $Ni_{0.9}Cu_{0.1}$ catalyst corresponds to a much higher a_C than the equilibrium for the Ni catalyst, in conflict with the results of the equilibrium studies in Ref.(*13*). Instead it can be suggested that adding Cu to Ni at the lower temperatures and lower a_C values diminish the rate strongly due to copper segregation on the surface. At the higher a_C values the segregation is partially reversed due to the fact that the chemisorption bonds between carbon and metal atoms are much stronger when the metal atom is nickel than when it is copper.

Enhancement of rates of reaction on nickel catalyst due to the addition of small amounts of copper have been reported before. Barcicki *et al.* (*22*) reported that very small amounts of Cu (0.02–0.1 at%) in Ni–Cu/Al$_2$O$_3$ catalysts strongly enhance the rate of methane steam reforming, while Cu contents of 1 at% or higher diminished the rate. A small part of the enhancement was ascribed to an increased reduction rate, while most of it was suggested to be due to a reduction of the self-poisoning of the catalysts. Van Barneveld and Ponec (*23*) and Martin and Dalmon (*24*) observed that copper addition to a Ni/SiO$_2$ catalyst enhances the hydrogenation of benzene at high temperatures. Tavares and Bernardo (*25*) observed that a $Ni_{0.99}Cu_{0.01}/SiO_2$ catalyst showed a higher rate of CO methanation than the corresponding Ni/SiO$_2$ catalyst and higher than Ni–Cu catalysts with higher Cu contents. More investigations are required to fully understand this promotion effect.

The Arrhenius plot of the slopes of the linearized kinetic model with step (2) rate limiting in Fig. 9 gives with the assumptions about $\theta*$ an activation energy for k_2 of about 90 kJ/mol. This is far higher than the value (about 50 kJ/mol) derived from surface science experiments (*4*, *5*). This deviation is undoubtedly due to the assumption that only step (2) deviates from equilibrium, which is in conflict with the microkinetic modelling (*19*). Thus the "effective" activation energy usually determined from an Arrhenius plot of the overall carbon formation rate may in many cases be an ill-defined parameter from which it is very difficult or impossible to derive information about the mechanism of the reaction.

5. CONCLUSION

Various kinetic models for carbon formation on nickel surfaces exposed to CH_4 + H_2 gas mixtures have been tested on the results obtained for a Ni/SiO_2 catalyst. It is shown that the rates cannot be considered as a function solely of the temperature and the carbon activity of the gas. A Grabke-type model based on a rate-limiting dissociative chemisorption step and stepwise dehydrogenation of the chemisorbed methyl gives good agreement with the experimental rates for the Ni/SiO_2 catalyst. A more general microkinetic model shows, however, that also the first dehydrogenation step deviates significantly from equilibrium. This means that the activation energy of the rate constant for the chemisorption of methane cannot be determined from an Arrhenius plot of the overall rate. The model has also been used on results for a $Ni_{0.9}Cu_{0.1}/SiO_2$ and a $Ni_{0.99}Cu_{0.01}/SiO_2$ catalyst. The rates of carbon formation on the NiCu catalyst with 1% Cu are higher than the rates for the Ni catalyst. The rates for the 10% Cu catalyst are much smaller than the rates for the Ni catalyst and only the results corresponding to low carbon activities are in agreement with the kinetic model.

ACKNOWLEDGMENTS

M. T. Tavares wishes to thank Professor C. A. Bernardo for fruitful discussions. This work has been supported by the Danish Research Councils through the Center for Surface Reactivity. Visits of M. T. Tavares to the Haldor Topsøe Research Laboratories have been supported within the COMETT programme 89/4/2-051.

REFERENCES

1. Rostrup-Nielsen, J. R., *in* "Catalysis Science and Technology" (J. R. Anderson and M. Boudart, Eds.), Vol. 4, Chap. 1. Springer, Berlin, 1983.
2. Rostrup-Nielsen, J. R., and Alstrup, I., *in* "Studies in Surface Science and Catalysis" (J. W. Ward, Ed.), Vol. 38, p. 725. Elsevier, Amsterdam, 1988.
3. Lee, M. B., Yang, Q. Y., Tang, S. L., and Ceyer, S. T., *J. Chem. Phys.* **87,** 2724 (1987).
4. Beebe, T. P., Jr., Goodman, D. W., Kay, B. D., and Yates, J. T., Jr., *J. Chem. Phys.* **87,** 2305 (1987).
5. Chorkendorff, I., Alstrup, I., and Ullmann, S., *Surf. Sci.* **227,** 291 (1990).
6. Grabke, H. J., *Ber. Bunsenges. Phys. Chem.* **69,** 409 (1965).
7. Grabke, H. J., *Metall. Trans.* **1,** 2972 (1970).
8. Grabke, H. J., and Martin, E., *Arch. Eisenhuettenwes.* **44,** 837 (1973).
9. Grabke, H. J., Müller, E. M., and Konczos, G., *Scr. Metall.* **14,** 159 (1980).
10. Lázár, K., Kertész, K., Császár-Gilicze, É., and Konczos, G., *Z. Metallkd.* **71,** 124 (1980).
11. Figueiredo, J. L., and Trimm, D. L., *J. Catal.* **40,** 154 (1975).
12. Audier, M., and Coulon, M., *Carbon* **23,** 317 (1985).
13. Bernardo, C. A., Alstrup, I., and Rostrup-Nielsen, J. R., *J. Catal.* **96,** 517 (1985).
14. Baker, R. T. K., Harris, P. S., Thomas, R. B., and Waite, R. J., *J. Catal.* **30,** 86 (1973).
15. Rostrup-Nielsen, J. R., and Trimm, D. L., *J. Catal.* **48,** 155 (1977).
16. Safvi, S. A., Bianchini, E. C., and Lund, C. R. F., *Carbon* **29,** 1245 (1991).
17. Demicheli, M. C., Ponzi, E. N., Ferretti, O. A., and Yeramian, A. A., *Chem. Eng. J.* **46,** 129 (1991).
18. Tavares, M. T., Bernardo, C. A., Alstrup, I., and Rostrup-Nielsen, J. R., *J. Catal.* **100,** 545 (1986).

19. Alstrup, I., and Tavares, M. T., *J. Catal.* **135,** 147 (1992).
20. Bianchini, E. C., and Lund, C. R. F., *J. Catal.* **117,** 455 (1989).
21. Manning, M. P., Garmirian, J. E., and Reid, R. C., *Ind. Eng. Chem. Process Des. Dev.* **21,** 404 (1982).
22. Barcicki, J., Nazimek, D., Grzegorczyk, W., Borowiecki, T., and Denis, A., *Polish J. Chem.* **55,** 1839 (1981).
23. van Barneveld, W. A. A., and Ponec, V., *Rec. Trav. Chim.* **93,** 243 (1974).
24. Martin, G. A., and Dalmon, J. A., *J. Catal.* **75,** 233 (1982).
25. Tavares, M. T., and Bernardo, C. A., in preparation.